

Stanniocalcin1 knockdown induces ferroptosis and suppresses glycolysis in prostate cancer via the Nrf2 pathway

Yuan-Qing DAI^{1,2}, Yao BAI³, Jie GU¹, Ben-Yi FAN^{1,2,*}

¹Department of Urology, XiangYa Hospital, Central South University, Changsha, Hunan, China; ²National Clinical Research Center for Geriatric Disorders, Xiangya Hospital, Central South University, Changsha, Hunan, China; ³Department of Urology, Hunan Provincial People's Hospital, The First Affiliated Hospital of Hunan Normal University, Changsha, Hunan, China

*Correspondence: fanbenyi2022@yeah.net

Received June 26, 2022 / Accepted November 21, 2022

Stanniocalcin1 (STC1) is a secreted glycoprotein, which is highly expressed in prostate cancer cells. However, the biological functions of STC1 in modulating ferroptosis and glycolysis in prostate cancer are still not clear. The viability of PC-3 and DU145 cells was detected by CCK-8 assay. The relative Fe²⁺ level was detected by an Iron Assay Kit. MDA level was detected by Lipid Peroxidation MDA Assay Kit. Glucose uptake and lactate product were measured by Glycolysis Assay Kit and Lactate Assay Kit. In this study, STC1 was highly expressed in prostate cancer tissue specimens and cells. STC1 knockdown suppressed prostate cancer cell proliferation, and upregulated Fe²⁺ level, reduced glutathione (GSH) level, downregulated GPX4 and SLC7A11 protein expressions in PC-3 cells and DU145 cells. Besides, STC1 knockdown decreased glucose uptake, lactate product, and ATP level, as well as downregulated glycolysis-related protein HK2 and LDHA protein expressions. In addition, STC1 knockdown repressed the Nrf2/HO-1/NQO1 pathway. Nrf2 pathway activator, Oltipraz, upregulated Nrf2, total NQO1, and HO-1 expressions in PC-3 cells and DU145 cells. Moreover, Nrf2 pathway activator Oltipraz reversed the effect of STC1 knockdown on Fe²⁺ level and GPX4, SLC7A11, HK2, LDHA protein expressions in PC-3 cells and DU145 cells. Finally, STC1 knockdown restrained the tumor volume, tumor weight, and glycolysis in prostate cancer in vivo. Thus, STC1/Nrf2 pathway is a vital pathway to induce ferroptosis and suppress glycolysis in prostate cancer.

Key words: stanniocalcin 1, Nrf2, ferroptosis, glycolysis, prostate cancer

Prostate cancer is the main prevalent cancer in the male genital system, with 248,530 estimated new cases and 34,130 estimated deaths in 2021 in the USA [1]. For localized prostate cancer patients, surgery or radiation therapy can achieve satisfactory treatment effects [2]. The proliferation, growth, and differentiation of prostate cancer cells are dependent on androgens, so androgen deprivation therapy is the main treatment for advanced and metastatic prostate cancer patients [3, 4]. However, this treatment is transiently effective for advanced prostate cancer patients, and prostate cancer will eventually progress to castrate-resistant prostate cancer [5]. Therefore, it is essential to develop new methods and discover new targets for prostate cancer treatment.

Ferroptosis is a form of erastin-induced cell death that acts as a result of fatal lipid peroxidation, and it represses cystine import, causes glutathione (GSH) depletion, and glutathione peroxidase 4 (GPX4) inactivation [6]. Studies have reported that ferroptosis is related to cardiovascular diseases, neurological diseases, and cancer progression, moreover, it can act

as a tumor suppressor function [7–9]. In addition, researchers have identified the tumor suppression effect of ferroptosis in prostate cancer [10, 11]. Increased glycolysis is important for the viability, proliferation, and growth of cancer cells, which increases glucose uptake and lactate production [12, 13]. Studies have shown that sustained treatment of androgen can facilitate glucose uptake and lactate production in prostate cancer, therefore, androgen exerts a critical role in accelerating prostate cancer glycolysis [14]. Thus, ferroptosis exerts a tumor suppression function and glycolysis plays a cancer-promoting effect in prostate cancer.

Nrf2 is a vital transcriptional modulator, and its activation can repress oxidative stress and inflammation in cancer, such as hepatocellular carcinoma, bladder cancer, and breast cancer [15, 16]. Nrf2 increases glycolytic enzyme expressions to facilitate glycolytic flow, such as hexokinase 2 (HK2), pyruvate kinase muscle (PKM), and enolase 1 (ENO1) [17]. Researchers have reported that Nrf2 can facilitate glycolysis to enhance the growth of breast cancer cells [18]. A recent

study shows that repressing Nrf2 signaling can promote ferroptosis in prostate cancer cells [19]. Stanniocalcin1 (STC1) is a secreted glycoprotein, which promotes Nrf2 and HO-1 expression, and exerts anti-apoptotic function by promoting the Nrf2 pathway in acute kidney injury [20]. Our previous study has identified that STC1 is upregulated in prostate cancer cells, and STC1 knockdown represses prostate cancer cell proliferation *in vitro* and tumor growth *in vivo* [21]. However, whether STC1 regulates ferroptosis and glycolysis via Nrf2 in prostate cancer is not clear.

In this study, we identified the role of STC1 knockdown in the induction of ferroptosis and suppression of glycolysis in prostate cancer cells and revealed that STC1 exerted its function in ferroptosis and glycolysis in prostate cancer through the Nrf2 pathway.

Patients and methods

Tissue samples and cell culture. Sixty-eight pairs of prostate cancer tissues and adjacent tissues were received from prostate cancer patients when they underwent surgery at XiangYa hospital. Patients did not receive pre-operative treatments, such as radiotherapy or chemotherapy, and were confirmed by two histopathologists. Prostate cancer tissues were kept at -80°C . This study was approved by the Ethics Committee of XiangYa Hospital of Central South University, and informed consent was obtained from all participants.

Prostate cancer cell lines PC-3 (Shanghai Cell Bank of Chinese Academy of Sciences, catalog number: SCSP-532), DU145, VCaP, LNCaP, and human normal prostate epithelial cell line RWPE-1 were incubated in Dulbecco's Modified Eagle Medium (DMEM) (Gibco, CA, USA) with 10% fetal bovine serum (FBS; Gibco), 1% glutamax (Invitrogen, CA, USA), and 1% sodium pyruvate (Invitrogen) in a 5% CO_2 incubator at 37°C .

Short hairpin RNA (shRNA) targeting STC1 (sh-STC1#1, 5'-GCAGCAGCATCACCAGCAACA-3'; sh-STC1#2, 5'-GATCCACATCTTCACTCAAGC-3'; sh-STC1#3, 5'-TTAGTCCAGGAAGCAATAGTA3') and shRNA negative control (sh-NC, 5'-TTCTTTCGAAGGTGTACGT-3') were obtained from GENECHM (Shanghai, China). PC-3 and DU145 cells were transfected with plasmids using a Lipofectamine reagent (Invitrogen). Ferroptosis inhibitor ferrostatin-1, ferroptosis inducer erastin, and Nrf2 pathway activator Oltipraz were obtained from Sigma-Aldrich (MO, USA).

qRT-PCR. Total RNAs were isolated from prostate cancer tissues and cells with TRIzol reagent (Invitrogen). cDNA was synthesized using the PrimeScript 1st Strand cDNA Synthesis Kit (Takara, Beijing, China). Real-time PCR analyses were performed by One Step TB Green PrimeScrip PLUS RT-PCR Kit (Takara, Beijing, China) on a QuantStudio 5 Real Time System (ThermoFisher Scientific, CA, USA). Results were normalized to GAPDH expression. Primers for STC1 and GAPDH were shown as follows: STC1, forward

primer: 5'-GCAGGAAGAGTGCTACAGCAAG-3', reverse primer: 5'-CATTCAGCAGGCTTCGGACAA-3'; GAPDH, forward primer: 5'-AGAAGGCTGGGGCTCATTTG-3', reverse primer: 5'-AGGGGCCATCCACAGTCTTC-3'.

Western blotting. Prostate cancer tissues and cells were washed with cold PBS and lysed in RIPA buffer (Beyotime Biotechnology, Nantong, China). Proteins were analyzed by SDS-PAGE and transferred to the PVDF membrane. The blots were probed with primary antibodies at 4°C for 12 h: anti-STC1 (1:1000; Abcam, cat. number: ab229477), anti-GPX4 (1:1000; Cell Signaling Technology, cat. number: 59735), anti-SLC7A11 (1:1000; Cell Signaling Technology, cat. number: 12691), anti-HK2 (1:1000; Cell Signaling Technology, cat. number: 2867), anti-LDHA (1:1000; Cell Signaling Technology, cat. number: 3582), anti-Nrf2 (1:1000; Cell Signaling Technology, cat. number: 12721), anti-Lamin B1 (1:1000; Cell Signaling Technology, cat. number: 13435), anti-HO-1 (1:10000; Abcam, cat. number: ab68477), anti-NQO1 (1:1000; Cell Signaling Technology, cat. number: 62262), anti- β -actin (1:1000; Cell Signaling Technology, cat. number: 4970). The HRP-ECL method was applied for the evaluation of signal intensities in western blotting. The immunoreactive proteins were detected using an ECL kit (ThermoFisher Scientific, CA, USA) and quantified using iBright Imaging System (Invitrogen, CA, USA).

Cell counting kit-8 assay (CCK-8). CCK-8 assay kit (Beyotime Biotechnology, Nantong, China) was used to detect PC-3 and DU145 cells' viability. Cells (3×10^3) were seeded in 96-well plates and incubated for 24, 48, and 72 h. CCK-8 solution (10 μl) was added to each well. Optical density at 450 nm (OD450) was measured by a microplate reader (Bio-Rad, CA, USA).

Iron assay. The relative Fe^{2+} level in the cell lysate was detected by an Iron Assay Kit (Abcam). Fe^{2+} in the cell lysate reacted with Ferene S and incubated for 30 min at 37°C to produce a stable-colored complex. The absorbance at 593 nm was analyzed with a microplate reader (Bio-Rad).

Determination of Reactive Oxygen Species (ROS). ROS production was determined by 2,7-dichlorodihydrofluorescein diacetate (DCFH-DA; Sigma-Aldrich). PC-3 and DU145 cells (5×10^3 cells/well) were seeded in 96-well plates and incubated with $8 \mu\text{M}$ DCFH-DA for 15 min at 37°C . The fluorescence was measured with a microplate reader (Bio-Rad).

Lipid peroxidation malondialdehyde (MDA) assay. MDA level was detected by Lipid Peroxidation MDA Assay Kit (Beyotime Biotechnology). PC-3 and DU145 cell lysates were added with MDA detection solution, heated in a boiling water bath for 15 min, cooled to 25°C , and centrifuged at $1000 \times g$ at 25°C for 10 min. The absorbance at 532 nm was determined by a microplate reader (Bio-Rad).

GSH and GSSG assay. GSH level was determined using GSH and GSSG Assay Kit (Beyotime Biotechnology). PC-3 and DU145 cells precipitation was kept in the ice bath for 5 min, then centrifuged at $10,000 \times g$ at 4°C for 10 min. The

supernatant was used for the determination of total glutathione. Then, the GSH removal solution was added to total glutathione, and the absorbance at 412 nm was determined using a microplate reader (Bio-Rad) to determine the GSSG level. GSH level was calculated according to the formula: $GSH = Total\ Glutathione - GSSG \times 2$.

Glycolysis assay and ATP detection assay. Glucose uptake and lactate product were measured by Glycolysis Assay Kit (BioVision, CA, USA) and Lactate Assay Kit (BioVision). PC-3 and DU145 cells were seeded in 96-well plates (5×10^5 cells/well). A glycolysis assay reagent (10 μ l) was added to each well. The absorbance at 570 nm was determined using a microplate reader (Bio-Rad). ATP level was detected by Luminescent ATP Detection Assay (Abcam). Cells were added with a detergent solution and incubated for 5 min to lyse cells and stabilize ATP. Substrate solution was added and incubated for 5 min. After incubating in the dark for 10 min, the emitted light was determined by a luminescence plate reader (Promega, WI, USA).

Animal experiments. Six-week-old BALB/c nude mice were obtained from the laboratory animal center of Central South University. DU145 cells were transfected with sh-NC or sh-STC1. The 0.1 ml DU145 cell suspension including 5×10^6 cells was subcutaneously injected into the back of nude mice. During 5–30 days of injection, tumor volumes were recorded every five days according to the formula: $length \times width^2/2$. Besides, animal weight was recorded every five days. Mice were sacrificed at day 30 by an overdose of 100 mg/kg pentobarbital sodium via intravenous injection. This animal experiment was approved by the Ethics Committee of XiangYa Hospital of Central South University.

Immunohistochemistry staining (IHC). The paraffin-embedded tumor tissues were fixed, then incubated with primary antibodies anti-Ki-67 (1:200; Cell Signaling Technology, cat. number: 12202), anti-STC1 (1:100; Abcam, cat. number: ab229477), anti-GPX4 (1:50; Abcam, cat. number: ab125066), anti-HK2 (1:500; Abcam, cat. number: ab209847), anti-LDHA (1:200; Cell Signaling Technology, cat. number: 3582) at 4°C overnight, followed by a secondary antibody rabbit IgG (1:100; Abcam, cat. number: ab288151) for 60 min. Tissues were incubated with DAPI at 37°C for 15 min. Images were examined under a confocal microscope (Nikon, Japan).

Statistical analysis. All experiments were independently repeated three times. SPSS 20.0 software was used to analyze the data. Data were presented as mean \pm standard deviation. Differences between the two groups were assessed by Student's t-test. Differences for multiple groups were assessed by one-way analysis of variance (ANOVA) followed by the Bonferroni post hoc test. A p-value <0.05 was considered significant.

Results

STC1 was highly expressed in prostate cancer tissue specimens and cells. Previously, we found STC1 was upregulated in DU145 and LNCaP2 cells [21]. In this study, we further determined STC1 expression in prostate cancer tissue. mRNA expression of STC1 was elevated in prostate cancer tissue than in adjacent tissues (Figure 1A; $n=68$; $p<0.001$). In addition, we selected six pairs of prostate cancer tissues and adjacent tissues and determined that STC1 protein expres-

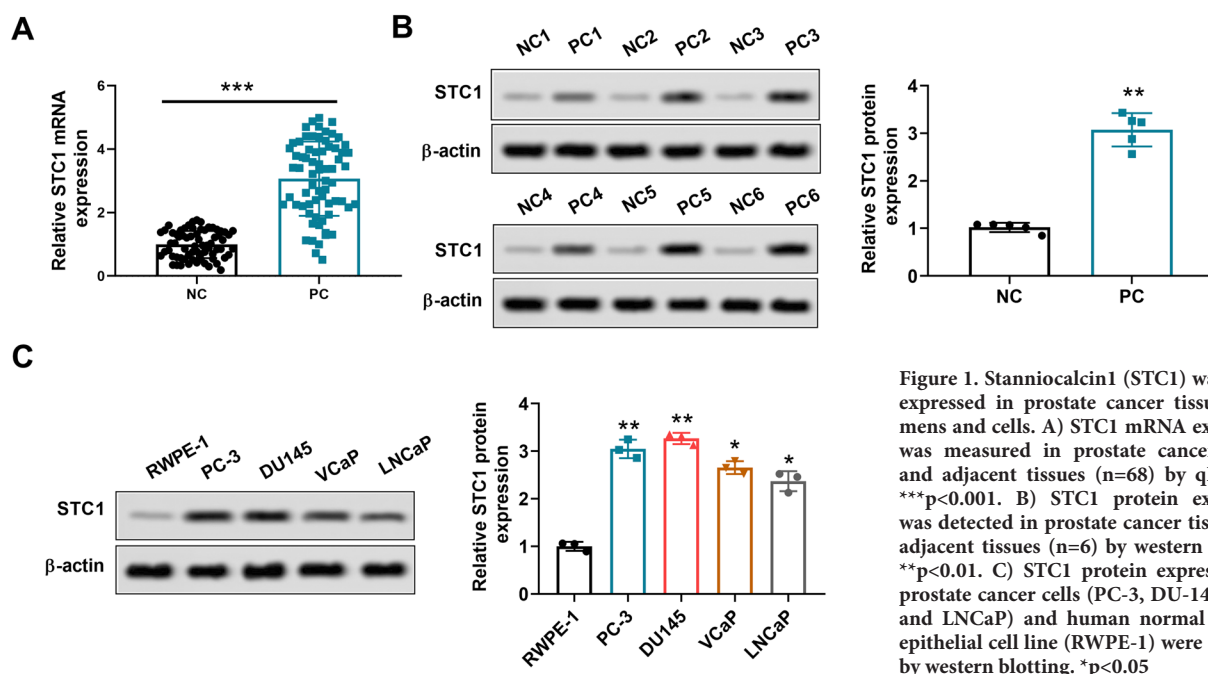


Figure 1. Stanniocalcin1 (STC1) was highly expressed in prostate cancer tissue specimens and cells. A) STC1 mRNA expression was measured in prostate cancer tissues and adjacent tissues ($n=68$) by qRT-PCR. $***p<0.001$. B) STC1 protein expression was detected in prostate cancer tissues and adjacent tissues ($n=6$) by western blotting. $**p<0.01$. C) STC1 protein expressions in prostate cancer cells (PC-3, DU-145, VCaP, and LNCaP) and human normal prostate epithelial cell line (RWPE-1) were analyzed by western blotting. $*p<0.05$

sion was markedly elevated in prostate cancer tissue than in adjacent tissues (Figure 1B; $p < 0.001$). Besides, STC1 protein expressions were dramatically upregulated in prostate cancer cells (PC-3, DU145, VCaP, and LNCaP) than normal RWPE-1 cells (Figure 1C; $p < 0.05$). According to the correlation analysis between STC1 expression and clinicopathological characteristics in prostate cancer, we found that the high STC1 expression was closely related to Gleason score, but not related to the age, T stage, metastasis, and invasion to partial vesicle (Table 1; $p < 0.05$). Therefore, STC1 expression was highly expressed in prostate cancer, which might be related to prostate cancer progression.

STC1 knockdown suppressed prostate cancer cell proliferation and induced ferroptosis in prostate cancer. sh-STC1#1, sh-STC1#2, and sh-STC1#3 were used to interfere STC1 expression in PC-3 cells and DU145 cells. We found that mRNA and protein expressions of STC1 were dramatically downregulated in the sh-STC1#1, sh-STC1#2, and sh-STC1#3 groups than in the control and sh-NC groups, and sh-STC1#1 achieved a better inhibition effect (PC-3 cells and DU145 cells; Figures 2A, 2B; $p < 0.01$). So, we used sh-STC1#1 for the following experiments and named it sh-STC1. According to the CCK-8 assay, we found that absorbance values (OD450) at 48 h and 72 h were markedly reduced in the sh-STC1 group than in the sh-NC group (PC-3 cells and DU145 cells; Figure 2C; $p < 0.01$). In addition, Fe^{2+} levels were observably increased in the sh-STC1 group than in the sh-NC group (PC-3 cells and DU145 cells; Figure 2D; $p < 0.01$). Moreover, after the treatment of ferroptosis inducer erastin, Fe^{2+} level was significantly upregulated in PC-3 cells and DU145 cells, whereas after the treatment of ferroptosis inhibitor ferrostatin-1, Fe^{2+} level was markedly decreased

in PC-3 cells and DU145 cells transfected with sh-STC1 (Figure 2E; $p < 0.05$). ROS level was dramatically increased in the sh-STC1 group than in the sh-NC group (PC-3 cells and DU145 cells; Figure 2F; $p < 0.01$). MDA level was observably elevated in the sh-STC1 group than in sh-NC (PC-3 cells and DU145 cells; Figure 2G; $p < 0.01$). GSH level was markedly repressed in the sh-STC1 group than in sh-NC (PC-3 cells and DU145 cells; Figure 2H; $p < 0.01$). Moreover, GPX4 and SLC7A11 protein expressions were dramatically decreased in the sh-STC1 group than in the sh-NC group (PC-3 cells and DU145 cells; Figure 2I; $p < 0.01$). Therefore, STC1 induced the proliferation and repressed ferroptosis in PC-3 cells and DU145 cells.

STC1 knockdown repressed glycolysis in prostate cancer. Since we have identified the effect of STC1 on ferroptosis in prostate cancer, the effect of STC1 on glycolysis was further investigated. Glucose uptake, lactate product, and ATP level were markedly reduced in the sh-STC1 group than in the sh-NC group (in PC-3 cells and DU145 cells; Figures 3A–3C; $p < 0.01$). Besides, glycolysis-related protein HK2 and LDHA protein expressions were dramatically reduced in the sh-STC1 group than in the sh-NC group (PC-3 cells and DU145 cells; Figure 3D; $p < 0.01$). Thus, STC1 induced glycolysis in PC-3 cells and DU145 cells.

STC1 knockdown induced ferroptosis and suppresses glycolysis in prostate cancer via Nrf2. Nrf2 induced glycolysis in breast cancer cells [18] and repressed ferroptosis in prostate cancer cells [19]. So, whether STC1 modulated the Nrf2 pathway in prostate cancer was investigated here. As shown in Figure 4A, Nrf2 in the nucleus, total NQO1, and HO-1 protein expressions were observably reduced in the sh-STC1 group than sh-NC (PC-3 cells and DU145 cells; $p < 0.01$), indicating STC1 knockdown repressed the Nrf2/HO-1/NQO1 pathway in prostate cancer. After the treatment of Nrf2 pathway activator Oltipraz (25 μ M), Nrf2 in the nucleus, total NQO1, and HO-1 protein expressions were significantly upregulated in DU145 cells transfected with sh-STC1 (Figure 4B; $p < 0.01$). Absorbance values (OD450) were increased in the sh-STC1+ Oltipraz group than in the sh-NC and sh-STC1 groups at 48 h and 72 h (DU145 cells; Figure 4C; $p < 0.01$). Fe^{2+} level in DU145 cells was observably reduced in the sh-STC1+ Oltipraz group than in the sh-NC and sh-STC1 groups (Figure 4D). ROS level was markedly repressed in the sh-STC1+ Oltipraz group than in the sh-NC and sh-STC1 groups (DU145 cells; Figures 4E, 4F). GPX4, SLC7A11, HK2, and LDHA protein expressions were dramatically elevated in the sh-STC1+ Oltipraz group than in the sh-NC and sh-STC1 groups (DU145 cells; Figure 4G). Thus, STC1 positively modulated the Nrf2 pathway in prostate cancer to induce glycolysis and repress ferroptosis.

STC1 knockdown suppresses the proliferation and glycolysis in prostate cancer *in vivo*. To further verify this observation, an animal experiment was conducted by subcutaneous injection of DU145 cells (5×10^6) into nude mice, with five mice in each group. Tumor volume was markedly

Table 1. Correlation between STC1 expression and the clinical pathological features of 68 prostate cancer patients.

| Characteristic | All cases | STC1 expression | | p-value |
|-----------------------------|-----------|-----------------|------------|---------|
| | | High (n=34) | Low (n=34) | |
| Age (years) | | | | 0.168 |
| <60 | 26 | 14 | 12 | |
| ≥ 60 | 42 | 20 | 22 | |
| Gleason score | | | | 0.028* |
| <7 | 29 | 11 | 20 | |
| ≥ 7 | 39 | 23 | 14 | |
| T stage | | | | 0.625 |
| T 1–2 | 30 | 14 | 16 | |
| T 3–4 | 38 | 20 | 18 | |
| Metastasis to lymph nodes | | | | 0.457 |
| Yes | 27 | 15 | 12 | |
| No | 41 | 19 | 22 | |
| Invasion to seminal vesicle | | | | 0.622 |
| Yes | 40 | 21 | 19 | |
| No | 28 | 13 | 15 | |

Note: * $p < 0.05$

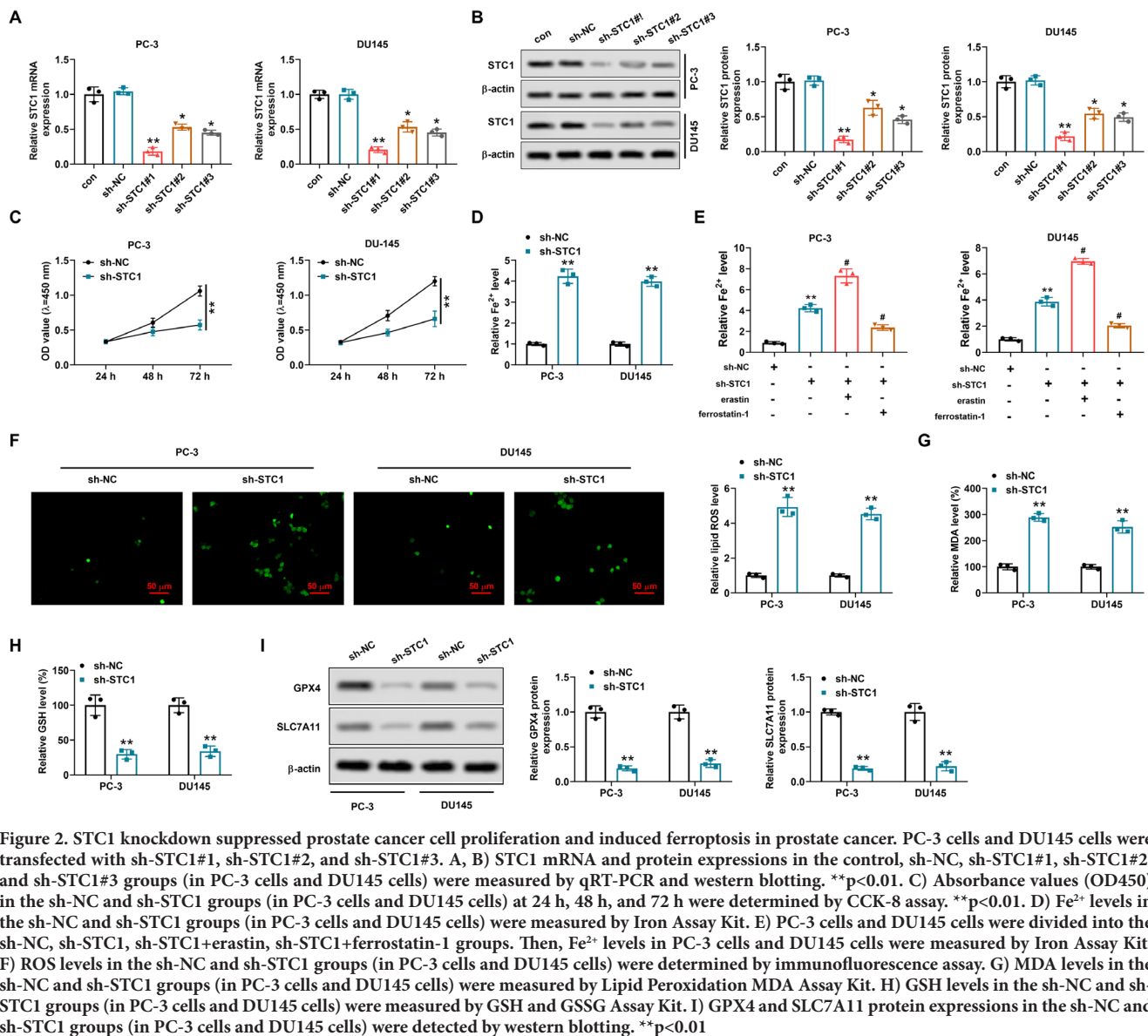


Figure 2. STC1 knockdown suppressed prostate cancer cell proliferation and induced ferroptosis in prostate cancer. PC-3 cells and DU145 cells were transfected with sh-STC1#1, sh-STC1#2, and sh-STC1#3. **A, B**) STC1 mRNA and protein expressions in the control, sh-NC, sh-STC1#1, sh-STC1#2, and sh-STC1#3 groups (in PC-3 cells and DU145 cells) were measured by qRT-PCR and western blotting. **p<0.01. **C**) Absorbance values (OD450) in the sh-NC and sh-STC1 groups (in PC-3 cells and DU145 cells) at 24 h, 48 h, and 72 h were determined by CCK-8 assay. **p<0.01. **D**) Fe²⁺ levels in the sh-NC and sh-STC1 groups (in PC-3 cells and DU145 cells) were measured by Iron Assay Kit. **E**) PC-3 cells and DU145 cells were divided into the sh-NC, sh-STC1, sh-STC1+erastin, sh-STC1+ferrostatin-1 groups. Then, Fe²⁺ levels in PC-3 cells and DU145 cells were measured by Iron Assay Kit. **F**) ROS levels in the sh-NC and sh-STC1 groups (in PC-3 cells and DU145 cells) were determined by immunofluorescence assay. **G**) MDA levels in the sh-NC and sh-STC1 groups (in PC-3 cells and DU145 cells) were measured by Lipid Peroxidation MDA Assay Kit. **H**) GSH levels in the sh-NC and sh-STC1 groups (in PC-3 cells and DU145 cells) were measured by GSH and GSSG Assay Kit. **I**) GPX4 and SLC7A11 protein expressions in the sh-NC and sh-STC1 groups (in PC-3 cells and DU145 cells) were detected by western blotting. **p<0.01

reduced in the sh-STC1 group than in the sh-NC group (Figure 5A). No significant difference was observed in mice weight between the sh-NC and sh-STC1 groups (Figure 5B), whereas tumor weight was observably decreased in the sh-STC1 group than in the sh-NC group (Figure 5C). Ki-67, STC1, GPX4, SLC7A11, HK2, and LDHA tumor expressions (percentage of tumor cells staining for Ki-67, STC1, GPX4, SLC7A11, HK2, and LDHA) by IHC assay were markedly reduced in the sh-STC1 group than in the sh-NC group (Figure 5D). Nrf2 in the nucleus, total NQO1, and HO-1 protein expressions were dramatically reduced in the sh-STC1 group than in the sh-NC group (Figure 5E). Taken together, STC1 facilitated the growth and glycolysis of prostate cancer in an animal experiment.

Discussion

STC1 is a secreted glycoprotein that can modulate calcium and phosphate homeostasis in plasma [22]. STC1 is highly expressed in cancer tissues and cells and exerts an oncogenic function in many cancers [23]. For example, STC1 expression is elevated in colorectal cancer, and the deficiency of STC1 in fibroblasts decreases the infiltration of tumor cells and the formation of distant metastasis [23]. STC1 is highly expressed in ovarian cancer cells, and the inhibition of STC1 expression by sevoflurane represses ovarian cancer cell proliferation and invasion [24]. Our previous report showed that STC1 expression was elevated in prostate cancer cells and STC1 knockdown repressed prostate cancer cell proliferation

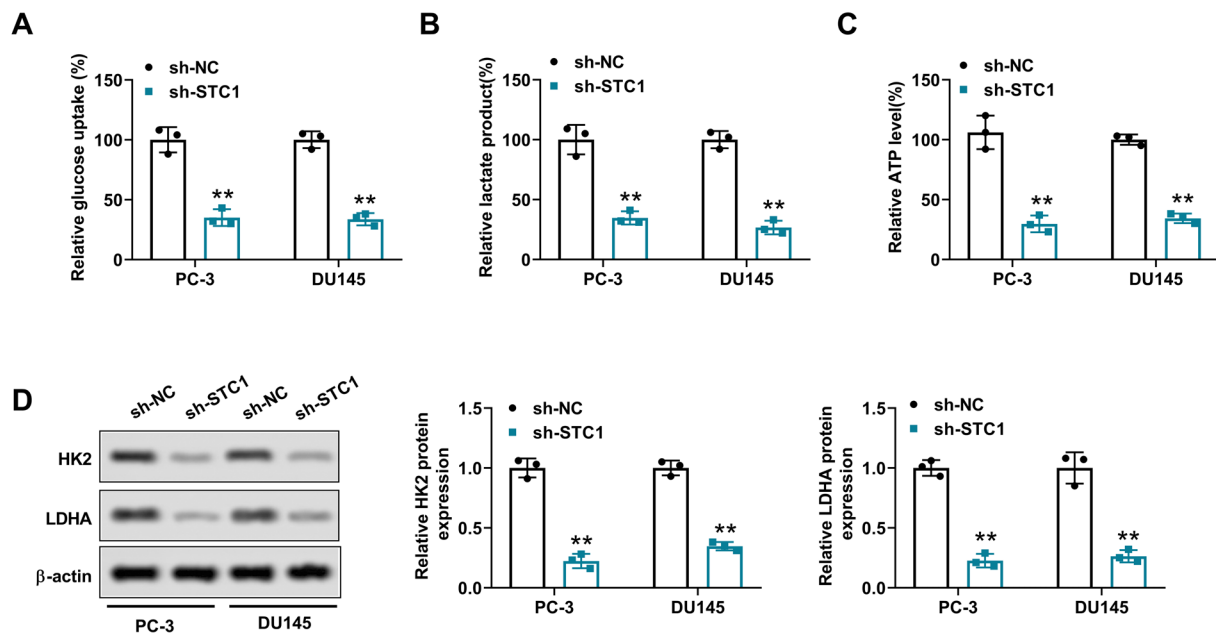


Figure 3. STC1 knockdown repressed glycolysis in prostate cancer. A–C) Glucose uptake, lactate product, and ATP level in the sh-NC and sh-STC1 groups (in PC-3 cells and DU145 cells) were determined by glycolysis assay and ATP detection assay. D) HK2 and LDHA protein expressions in the sh-NC and sh-STC1 groups (in PC-3 cells and DU145 cells) were measured by western blotting. ** $p < 0.01$

in vitro and tumor growth *in vivo* [21]. Costa et al. found that STC1 expression was elevated in more aggressive prostate cancer tissues, and anti-STC1 antibody repressed PC-3 cell proliferation and facilitated cell apoptosis [25]. In this study, mRNA and protein expressions of STC1 were elevated in prostate cancer tissues and cells lines (PC-3, DU145, VCaP, LNCaP), which indicated that the elevated STC1 might exert an oncogenic function in prostate cancer.

Ferroptosis is an adaptive characteristic that can remove malignant cells, which exerts a key function in inhibiting tumorigenesis by eliminating cells that lack critical nutrients or are injured due to infection or environmental stress [26]. Ferroptosis is mainly caused by extramitochondrial lipid peroxidation due to the increase of ROS [27]. It is a tumor protein p53-mediated activity, which is negatively modulated by SLC7A11 and GPX4 during tumor suppression [28, 29]. Researchers have shown that the treatment of ferroptosis inducers (erastin and RSL3) could increase ROS levels, reduce the proliferation, invasion, and migration of PC-3 and DU145 cells *in vitro*, and repress tumor growth *in vivo* [30]. Ferroptosis-related genes SLC7A11 and GPX4 expressions were repressed by Flubendazole in PC-3 and DU145 cells, which showed a vital role of ferroptosis in castration-resistant prostate cancer [10]. However, whether STC1 modulates ferroptosis in prostate cancer is not revealed. In this study, STC1 knockdown promoted Fe^{2+} level, sh-STC1+erastin further promoted Fe^{2+} level, and sh-STC1+erastatin-1 decreased Fe^{2+} level in PC-3 and DU145 cells. Moreover, STC1 knockdown increased ROS level and MDA level,

decreased GSH level, GPX4 and SLC7A11 expressions in PC-3 and DU145 cells. These findings identified that STC1 knockdown induced ferroptosis in prostate cancer.

Glycolysis is a prominent characteristic of cancer cells that exerts a vital function in the proliferation, migration, invasion, and drug resistance of cancer cells [31]. Although the efficiency of glycolysis is low, glycolysis is active in cancer cells because it can promptly generate more energy and metabolites [32]. Researchers have shown that enhanced glycolysis was exhibited in androgen-independent prostate cancer cells, and the inhibition of glycolysis in prostate cancer cells repressed tumor growth [33, 34]. Ohkouchi et al. found that mesenchymal stromal cells-derived STC1 enhanced glycolysis and increased lactate production in lung cancer [35]. In this study, STC1 knockdown reduced glucose uptake, lactate product, and ATP level, downregulated glycolysis-related protein HK2 and LDHA expressions in PC-3 cells and DU145 cells. These findings confirmed that STC1 knockdown repressed glycolysis in prostate cancer.

Nrf2 is a vital modulator in antioxidant response which promotes glutathione level and reduces ROS level [36]. Fan et al. showed that Nrf2 overexpressing gliomas were less sensitive to ferroptosis inducers (erastin and RSL3), indicating Nrf2 reduced ferroptotic cell death [37]. Wiel et al. found that Nrf2 increased glucose uptake, glycolysis rates, and lactate secretion to facilitate glycolysis in lung cancer [38]. Moreover, STC1 promoted Nrf2 and HO-1 expression and exerted anti-apoptotic function by facilitating the Nrf2 pathway in acute kidney injury [20]. However, whether STC1 regulates ferro-

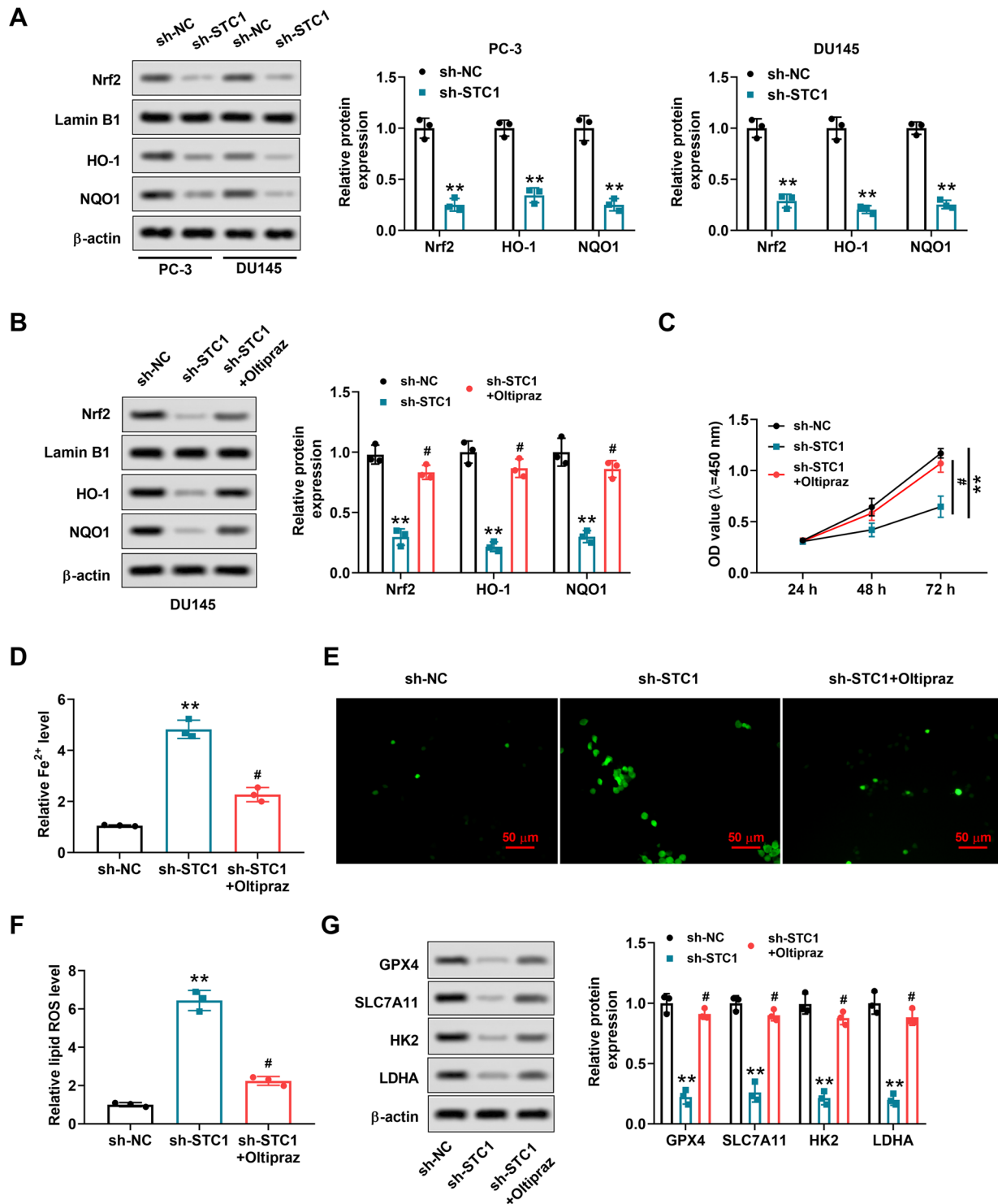


Figure 4. STC1 knockdown induced ferroptosis and suppresses glycolysis in prostate cancer via Nrf2. **A)** Nrf2 in the nucleus, total NQO1, and HO-1 protein expressions in the sh-NC and sh-STC1 groups (in PC-3 cells and DU145 cells) were measured by western blotting. ****p**<0.01. **B)** DU145 cells were divided into the sh-NC, sh-STC1, and sh-STC1+Oltipraz (25 μ M) groups. Nrf2 in the nucleus, total NQO1, and HO-1 protein expressions in DU145 cells were determined by western blotting. ****p**<0.01. **C)** Absorbance values (OD₄₅₀) in the three groups of DU145 cells at 24 h, 48 h, and 72 h were determined by the CCK-8 assay. ****p**<0.01 **D)** Fe²⁺ levels in the three groups of DU145 cells were measured by Iron Assay Kit. **E, F)** ROS levels in the three groups of DU145 cells were determined by immunofluorescence assay. **G)** GPX4, SLC7A11, HK2, and LDHA protein expressions in the three groups of DU145 cells were measured by western blotting. ****p**<0.01

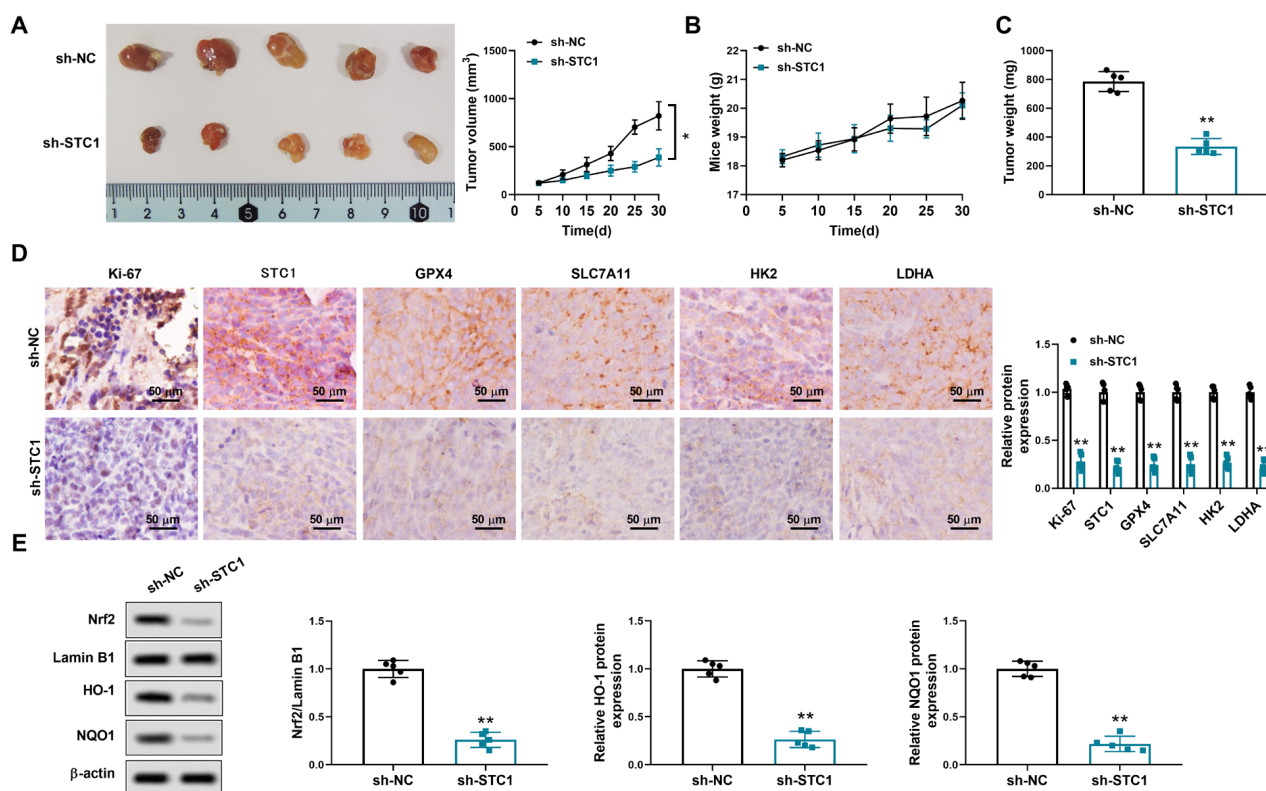


Figure 5. STC1 knockdown suppresses the proliferation and glycolysis in prostate cancer *in vivo*. DU145 cells transfected with sh-NC or sh-STC1 were subcutaneously injected into nude mice (n=5). **A**) Tumor volume was measured every five days for 30 days in the sh-NC and sh-STC1 groups. **B, C**) Mice weight was measured every five days for 30 days in the sh-NC and sh-STC1 groups. Then, all mice were sacrificed and tumor weight was recorded in the sh-NC and sh-STC1 groups. **D**) Ki-67, STC1, GPX4, SLC7A11, HK2, and LDHA expressions in the sh-NC and sh-STC1 groups by immunohistochemistry (IHC). **E**) Nrf2 in the nucleus, total NQO1, and HO-1 protein expressions in the sh-NC and sh-STC1 groups were determined by western blotting. **p<0.01

toxicity and glycolysis in prostate cancer is not illustrated. In this study, STC1 knockdown downregulated Nrf2, HO-1, and NQO1 protein expressions in PC-3 cells and DU145 cells, whereas Nrf2 pathway activator Oltipraz reversed the inhibition effect of STC1 knockdown on these protein expressions, which suggested that STC1 positively modulated the Nrf2 pathway in prostate cancer. In addition, STC1 knockdown increased Fe²⁺ level, ROS level, downregulated ferroptosis-related protein GPX4 and SLC7A11 expressions, and reduced glycolysis-related protein HK2 and LDHA expressions in DU145 cells. Whereas Oltipraz reversed the effect of STC1 knockdown on Fe²⁺ level, ROS level, and these protein expressions, indicating STC1 knockdown induced ferroptosis and suppressed glycolysis of prostate cancer via Nrf2.

STC1 knockdown can repress tumor growth of prostate cancer cell DU145 xenografts [21]. However, whether STC1 knockdown induced ferroptosis and suppressed glycolysis in prostate cancer *in vivo* was not investigated. In this *in vivo* animal study, STC1 knockdown reduced ferroptosis-related protein GPX4 and SLC7A11 expressions and decreased glycolysis-related protein HK2 and LDHA expressions in

prostate cancer tissues. Besides, STC1 knockdown repressed tumor weight and volume, downregulated proliferation marker Ki-67 expression, and suppressed the Nrf2 pathway. Thus, STC1 knockdown suppresses the growth and glycolysis and induced ferroptosis in prostate cancer *in vivo* xenograft model.

Taken together, our data identified STC1 knockdown suppressed cancer cell proliferation, induced ferroptosis, and repressed glycolysis in prostate cancer via the Nrf2 pathway *in vitro*, as well as suppressed tumor growth and glycolysis, and facilitated ferroptosis in prostate cancer *in vivo*. However, we only initially revealed the role of STC1 knockdown and its downstream molecules in prostate cancer. The upstream molecules in the modulation of STC1 are not investigated in this study. So, more experiments will be conducted to illustrate the underlying mechanism of STC1 in modulating ferroptosis and glycolysis in prostate cancer.

Acknowledgments: This study was supported by the Natural Science Foundation of Hunan Provincial (Grant Number 444885014-2018JJ3840/01).

References

- [1] SIEGEL RL, MILLER KD, FUCHS HE, JEMAL A. Cancer Statistics, 2021. *CA Cancer J Clin* 2021; 71: 7–33. <https://doi.org/10.3322/caac.21654>
- [2] MORGAN SC, HOFFMAN K, LOBLAW DA, BUYYOU-NOUSKI MK, PATTON C et al. Hypofractionated Radiation Therapy for Localized Prostate Cancer: Executive Summary of an ASTRO, ASCO and AUA Evidence-Based Guideline. *J Urol* 2019; 201: 528–534. <https://doi.org/10.1097/JU.0000000000000071>
- [3] LONERGAN PE, TINDALL DJ. Androgen receptor signaling in prostate cancer development and progression. *J Carcinog* 2011; 10: 20. <https://doi.org/10.4103/1477-3163.83937>
- [4] KATZENWADEL A, WOLF P. Androgen deprivation of prostate cancer: Leading to a therapeutic dead end. *Cancer Lett* 2015; 367: 12–17. <https://doi.org/10.1016/j.canlet.2015.06.021>
- [5] HALABI S, DUTTA S, TANGEN CM, ROSENTHAL M, PETRYLAK DP et al. Overall Survival of Black and White Men With Metastatic Castration-Resistant Prostate Cancer Treated With Docetaxel. *J Clin Oncol* 2019; 37: 403–410. <https://doi.org/10.1200/JCO.18.01279>
- [6] STOCKWELL BR, FRIEDMANN ANGELI JP, BAYIR H, BUSH AI, CONRAD M et al. Ferroptosis: A Regulated Cell Death Nexus Linking Metabolism, Redox Biology, and Disease. *Cell* 2017; 171: 273–285. <https://doi.org/10.1016/j.cell.2017.09.021>
- [7] CUI Y, ZHANG Y, ZHAO X, SHAO L, LIU G et al. ACSL4 exacerbates ischemic stroke by promoting ferroptosis-induced brain injury and neuroinflammation. *Brain Behav Immun* 2021; 93: 312–321. <https://doi.org/10.1016/j.bbi.2021.01.003>
- [8] BAO WD, PANG P, ZHOU XT, HU F, XIONG W et al. Loss of ferroportin induces memory impairment by promoting ferroptosis in Alzheimer's disease. *Cell Death Differ* 2021; 28: 1548–1562. <https://doi.org/10.1038/s41418-020-00685-9>
- [9] XU T, DING W, JI X, AO X, LIU Y et al. Molecular mechanisms of ferroptosis and its role in cancer therapy. *J Cell Mol Med* 2019; 23: 4900–4912. <https://doi.org/10.1111/jcmm.14511>
- [10] ZHOU X, ZOU L, CHEN W, YANG T, LUO J et al. Flubendazole, FDA-approved anthelmintic, elicits valid antitumor effects by targeting P53 and promoting ferroptosis in castration-resistant prostate cancer. *Pharmacol Res* 2021; 164: 105305. <https://doi.org/10.1016/j.phrs.2020.105305>
- [11] NASSAR ZD, MAH CY, DEHAIRS J, BURVENICH IJ, IRANI S et al. Human DECR1 is an androgen-repressed survival factor that regulates PUFA oxidation to protect prostate tumor cells from ferroptosis. *Elife* 2020; 9: e54166. <https://doi.org/10.7554/eLife.54166>
- [12] ZHAO X, WU X, WANG H, YU H, WANG J. USP53 promotes apoptosis and inhibits glycolysis in lung adenocarcinoma through FKBP51-AKT1 signaling. *Mol Carcinog* 2020; 59: 1000–1011. <https://doi.org/10.1002/mc.23230>
- [13] ZHAO X, TIAN Z, LIU L. circATP2B1 Promotes Aerobic Glycolysis in Gastric Cancer Cells Through Regulation of the miR-326 Gene Cluster. *Front Oncol* 2021; 11: 628624–628624. <https://doi.org/10.3389/fonc.2021.628624>
- [14] AUDET-WALSH É, YEE T, MCGUIRK S, VERNIER M, OUELLET C et al. Androgen-Dependent Repression of ERR γ Reprograms Metabolism in Prostate Cancer. *Cancer Res* 2017; 77: 378. <https://doi.org/10.1158/0008-5472.CAN-16-1204>
- [15] HE F, ANTONUCCI L, KARIN M. NRF2 as a regulator of cell metabolism and inflammation in cancer. *Carcinogenesis* 2020; 41: 405–416. <https://doi.org/10.1093/carcin/bgaa039>
- [16] BARTOLINI D, DALLAGLIO K, TORQUATO P, PIRODDI M, GALLI F. Nrf2-p62 autophagy pathway and its response to oxidative stress in hepatocellular carcinoma. *Transl Res* 2018; 193: 54–71. <https://doi.org/10.1016/j.trsl.2017.11.007>
- [17] FU J, XIONG Z, HUANG C, LI J, YANG W et al. Hyperactivity of the transcription factor Nrf2 causes metabolic reprogramming in mouse esophagus. *J Biol Chem* 2019; 294: 327–340. <https://doi.org/10.1074/jbc.RA118.005963>
- [18] ZHANG HS, DU GY, ZHANG ZG, ZHOU Z, SUN HL et al. NRF2 facilitates breast cancer cell growth via HIF1 α -mediated metabolic reprogramming. *Int J Biochem Cell Biol* 2018; 95: 85–92. <https://doi.org/10.1016/j.biocel.2017.12.016>
- [19] LIAO D, YANG G, YANG Y, TANG X, HUANG H et al. Identification of Pannexin 2 as a Novel Marker Correlating with Ferroptosis and Malignant Phenotypes of Prostate Cancer Cells. *Onco Targets Ther* 2020; 13: 4411–4421. <https://doi.org/10.2147/OTT.S249752>
- [20] ZHAO F, FENG LX, LIU Q, WANG HS, TANG CY et al. Stanniocalcin-1 Alleviates Contrast-Induced Acute Kidney Injury by Regulating Mitochondrial Quality Control via the Nrf2 Pathway. *Oxid Med Cell Longev* 2020; 2020: 1898213–1898213. <https://doi.org/10.1155/2020/1898213>
- [21] BAI Y, XIAO Y, DAI Y, CHEN X, LI D et al. Stanniocalcin 1 promotes cell proliferation via cyclin E1/cyclin-dependent kinase 2 in human prostate carcinoma. *Oncol Rep* 2017; 37: 2465–2471. <https://doi.org/10.3892/or.2017.5501>
- [22] CHEN F, ZHANG Z, PU F. Role of stanniocalcin-1 in breast cancer. *Oncol Lett* 2019; 18: 3946–3953. <https://doi.org/10.3892/ol.2019.10777>
- [23] PEÑA C, CÉSPEDES MV, LINDH MB, KIFLEMARIAM S, MEZHEYEUSKI A et al. STC1 Expression By Cancer-Associated Fibroblasts Drives Metastasis of Colorectal Cancer. *Cancer Res* 2013; 73: 1287. <https://doi.org/10.1158/0008-5472.CAN-12-1875>
- [24] ZHANG C, WANG B, WANG X, SHENG X, CUI Y. Sevoflurane inhibits the progression of ovarian cancer through down-regulating stanniocalcin 1 (STC1). *Cancer Cell Int* 2019; 19: 339–339. <https://doi.org/10.1186/s12935-019-1062-0>
- [25] COSTA BP, SCHEIN V, ZHAO R, SANTOS AS, KLIEMANN LM et al. Stanniocalcin-1 protein expression profile and mechanisms in proliferation and cell death pathways in prostate cancer. *Mol Cell Endocrinol* 2020; 502: 110659. <https://doi.org/10.1016/j.mce.2019.110659>
- [26] FEARNHEAD HO, VANDENABEELE P, VANDEN BERGHE T. How do we fit ferroptosis in the family of regulated cell death? *Cell Death Differ* 2017; 24: 1991–1998. <https://doi.org/10.1038/cdd.2017.149>

- [27] GAO M, MONIAN P, QUADRI N, RAMASAMY R, JIANG X. Glutaminolysis and Transferrin Regulate Ferroptosis. *Mol Cell* 2015; 59: 298–308. <https://doi.org/10.1016/j.molcel.2015.06.011>
- [28] LUO M, WU L, ZHANG K, WANG H, ZHANG T et al. miR-137 regulates ferroptosis by targeting glutamine transporter SLC1A5 in melanoma. *Cell Death Differ* 2018; 25: 1457–1472. <https://doi.org/10.1038/s41418-017-0053-8>
- [29] JIANG L, KON N, LI T, WANG SJ, SU T et al. Ferroptosis as a p53-mediated activity during tumour suppression. *Nature* 2015; 520: 57–62. <https://doi.org/10.1038/nature14344>
- [30] GHOOCHANI A, HSU EC, ASLAN M, RICE MA, NGUYEN HM et al. Ferroptosis Inducers Are a Novel Therapeutic Approach for Advanced Prostate Cancer. *Cancer Res* 2021; 81: 1583–1594. <https://doi.org/10.1158/0008-5472.CAN-20-3477>
- [31] CASCONI T, MCKENZIE JA, MBOFUNG RM, PUNT S, WANG Z et al. Increased Tumor Glycolysis Characterizes Immune Resistance to Adoptive T Cell Therapy. *Cell Metab* 2018; 27: 977–987.e974. <https://doi.org/10.1016/j.cmet.2018.02.024>
- [32] CAI L, HU C, YU S, LIU L, YU X et al. Identification and validation of a six-gene signature associated with glycolysis to predict the prognosis of patients with cervical cancer. *BMC Cancer* 2020; 20: 1133–1133. <https://doi.org/10.1186/s12885-020-07598-3>
- [33] LIANG T, YE X, YAN D, DENG C, LI Z et al. FAM46B Promotes Apoptosis and Inhibits Glycolysis of Prostate Cancer Through Inhibition of the MYC-LDHA Axis. *Onco Targets Ther* 2020; 13: 8771–8782. <https://doi.org/10.2147/OTT.S258724>
- [34] XIA L, SUN J, XIE S, CHI C, ZHU Y et al. PRKAR2B-HIF-1 α loop promotes aerobic glycolysis and tumour growth in prostate cancer. *Cell Prolif* 2020; 53: e12918–e12918. <https://doi.org/10.1111/cpr.12918>
- [35] OHKOUCHI S, BLOCK GJ, KATSHA AM, KANEHIRA M, EBINA M et al. Mesenchymal stromal cells protect cancer cells from ROS-induced apoptosis and enhance the Warburg effect by secreting STC1. *Mol Ther* 2012; 20: 417–423. <https://doi.org/10.1038/mt.2011.259>
- [36] DODSON M, CASTRO-PORTUGUEZ R, ZHANG DD. NRF2 plays a critical role in mitigating lipid peroxidation and ferroptosis. *Redox Biol* 2019; 23: 101107–101107. <https://doi.org/10.1016/j.redox.2019.101107>
- [37] FAN Z, WIRTH AK, CHEN D, WRUCK CJ, RAUH M et al. Nrf2-Keap1 pathway promotes cell proliferation and diminishes ferroptosis. *Oncogenesis* 2017; 6: e371–e371. <https://doi.org/10.1038/oncsis.2017.65>
- [38] WIEL C, LE GAL K, IBRAHIM MX, JAHANGIR CA, KASHIF M et al. BACH1 Stabilization by Antioxidants Stimulates Lung Cancer Metastasis. *Cell* 2019; 178: 330–345.e322. <https://doi.org/10.1016/j.cell.2019.06.005>